Bounding *CPT* violation in the neutral *B* system

V. Alan Kostelecký and R. Van Kooten

Physics Department, Indiana University, Bloomington, Indiana 47405

(Received 29 May 1996)

The feasibility of placing bounds on *CPT* violation from experiments with neutral *B* mesons is examined. We consider situations with uncorrelated mesons and ones with either unboosted or boosted correlated mesons. Analytical expressions valid for small *T*- and *CPT*-violating parameters are presented for time-dependent and time-integrated decay rates, and various relevant asymmetries are derived. We use Monte Carlo simulations to model experimental conditions for a plausible range of *CPT*-violating parameters. The treatment uses realistic data incorporating background effects, resolutions, and acceptances for typical detectors at CERN LEP, CESR, and the future *B* factories. Presently, there are no bounds on *CPT* violation in the *B* system. We demonstrate that limits of order 10% on *CPT* violation can be obtained from data already extant, and we determine the *CPT* reach attainable within the next few years. [S0556-2821(96)00321-9]

PACS number(s): 11.30.Er, 13.20.Fc, 13.20.Gd

I. INTRODUCTION

With the advent of experiments capable of reconstructing relatively large numbers of decays of neutral *B* mesons, a new window has opened for high-precision tests using the interferometric nature of the neutral *B* system in analogy to the neutral-kaon system. A particularly interesting possibility is testing *CPT* invariance, which is believed to be a fundamental symmetry of local relativistic particle field theories [1–7] and therefore also of the standard model. The possibility that *CPT* invariance might be spontaneously violated in string theory at observable levels via a mechanism arising as an indirect effect of string nonlocality has been suggested in Refs. [8–10]. *CPT* violation might also arise if quantum mechanics is modified by gravity [11–13], including perhaps in the context of string theory with unconventional quantum mechanics [14].

At present, the tightest bounds on *CPT* violation come from observations in the neutral-kaon system [15–18]. However, experimental bounds could also be obtained using other neutral-meson systems. This possibility is of interest because the magnitudes of *CPT* violation could be different in the various systems. For example, in the string scenario with spontaneous *CPT* violation, effects of different magnitude could appear at levels accessible to future and perhaps even present experiments not only in the *K* system but also in the *B* and *D* systems [10]. It has recently been demonstrated that *CPT* signals can in principle be separated from other effects in the neutral-*B* system using *B* factories [19] and in the neutral-*D* system using both correlated and uncorrelated decays [20]. These analyses were purely theoretical, disregarding background effects and detector acceptances. Otherwise, with a few notable exceptions [21,22], the issue of *CPT* violation in the *B* system has received relatively little attention in the literature. At present, there are no experimental limits on *CPT* violation in either the *B* or the *D* systems.

Several types of experiments collecting *B* events are presently underway or under construction. Close to 10^6 reconstructed uncorrelated *B* events are already available from each of the LEP collaborations [23]. Large numbers of un-

correlated *B* events have also been collected at the Fermilab Tevatron [24]. A symmetric *B* factory using the Cornell Electron Storage Ring (CESR) has produced relatively large numbers of correlated B_d^0-$\bar{B}_d^0$ pairs from the decay of the $\Upsilon(4S)$ resonance, with about 2.6×10^6 reconstructed $\Upsilon(4S)$ decay events obtained in CLEO [25]. Asymmetric *B* factories, which generate boosted correlated *B* pairs, are under construction at SLAC and KEK. The corresponding detectors BaBar and BELLE should provide approximately 10^7 reconstructed *B* pairs in a year at design luminosity [26].

In the present work, we investigate the practicability of extracting bounds on *CPT* violation from a variety of realistic experimental situations. We obtain analytical expressions for time-dependent and time-integrated decay rates that hold under general circumstances for uncorrelated, correlated unboosted, and correlated boosted *B* mesons. In each case, we use Monte Carlo simulations to provide a measure of the level at which *CPT* violation can be bounded. For definiteness, we perform simulations assuming a typical e^+e^- collider such as the LEP detector (OPAL) at CERN [27], the detector CLEO at CESR [28], and the detector BaBar at SLAC [29].

Our basic notation and conventions are presented in Sec. II, along with an outline of the procedure we adopt for the Monte Carlo simulations. We begin the detailed analysis in Sec. III, which treats the case of uncorrelated *B* mesons. The theory for this situation is in Sec. III A, while the experimental simulation involving the detector OPAL at CERN is in Sec. III B. Section IV discusses the case with correlated *B* mesons. The theoretical analysis is in Sec. IV A, and the experimental simulations for the unboosted (CLEO at CESR) and the boosted (BaBar at SLAC) situations are in Secs. IV B and IV C, respectively. Section V contains a summary.

II. PRELIMINARIES

This section contains basic definitions underlying our analyses and an outline of our simulation procedures. Most of our conventions are related to canonical ones for the kaon system and are discussed in more detail in Refs. [10,19]. Our analysis assumes throughout that any *CP* violation is small,

<u>54</u>   5585

which implies small T and CPT violation and it disregards terms that are higher order in small quantities.

The effective Hamiltonian for the B^0-$\bar{B}^0$ system has eigenvectors given by

$$|B_S\rangle = [(1 + \epsilon_B + \delta_B)|B^0\rangle + (1 - \epsilon_B - \delta_B)|\bar{B}^0\rangle]/\sqrt{2},$$

$$|B_L\rangle = [(1 + \epsilon_B - \delta_B)|B^0\rangle - (1 - \epsilon_B + \delta_B)|\bar{B}^0\rangle]/\sqrt{2}. \quad (1)$$

The quantities ϵ_B and δ_B are complex and parametrize CP violation. The former measures indirect T violation, while the latter measures indirect CPT violation. The analogous parameters ϵ_K and δ_K for the K system are defined by Eq. (1) but with the replacement $B \rightarrow K$.

The time evolution of the physical states B_S, B_L is governed by the corresponding eigenvalues of the effective Hamiltonian:

$$|B_S(t)\rangle = \exp(-im_S t - \gamma_S t/2)|B_S\rangle,$$

$$|B_L(t)\rangle = \exp(-im_L t - \gamma_L t/2)|B_L\rangle, \quad (2)$$

where the physical masses are m_S, m_L and the decay rates are γ_S, γ_L. It is convenient to introduce definitions for certain frequently occurring combinations of these quantities. We set

$$m = m_S + m_L, \quad \gamma = \gamma_S + \gamma_L,$$

$$\Delta m = m_L - m_S, \quad \Delta\gamma = \gamma_S - \gamma_L,$$

$$a^2 = \Delta m^2 + \Delta\gamma^2/4, \quad b^2 = \Delta m^2 + \gamma^2/4,$$

$$x = \frac{2\Delta m}{\gamma}, \quad y = \frac{\Delta\gamma}{\gamma}. \quad (3)$$

Experimental data are available for some of these quantities [30], specifically for the B_d^0 meson [31]. The mass difference is $|\Delta m_d| = (3.4 \pm 0.3) \times 10^{-13}$ GeV, and the mean lifetime is $\bar{\tau}_{B^0} = (1.50 \pm 0.11) \times 10^{-12}$ s. These values determine the magnitude of the mixing parameter x as $|x_d| \gtrsim 0.71 \pm 0.06$. We introduce the inequality here to allow for nonzero CPT violation, which affects the standard analysis [21] and increases the numerical value of $|x_d|$.

In contrast, no experimental limit exists on the scaled rate difference y. It is theoretically plausible to take the magnitude of y as $|y| \simeq 10^{-2} \ll |x|$. This estimate is based on the box diagram in perturbation theory, where the dominant intermediate states are the top and charm quarks. It is likely to be a good approximation since short-distance effects are larger than dispersive ones in the neutral-B system. More details about this analysis and references to the literature can be found in, for example, the reviews [32–35].

For the purposes of the present work, we focus on two types of B^0-decay modes: the semileptonic modes $B^0 \rightarrow D^{(*)}\ell\nu$ with ℓ being e or μ only, and the mode $B^0 \rightarrow J/\psi K_S$. These are particularly attractive from the experimental viewpoint. In principle, our CPT analyses could be further enhanced by grouping together certain special B decays, called *semileptonic-type* decays [19]. These include the standard semileptonic decays above, together with a subset of other modes $B^0 \rightarrow f$ for which there is no lowest-order

weak process allowing a significant contamination of either $\bar{B}^0 \rightarrow f$ or $B^0 \rightarrow \bar{f}$. Observed semileptonic-type decays include $B^0 \rightarrow D^- D_s^+$, $B^0 \rightarrow J/\psi K^+ \pi^-$, $B^0 \rightarrow J/\psi K^{*0}(892)$, $B^0 \rightarrow \psi(2S)K^{*0}(892)$, and similar decays into excited states [30]. Observed modes other than those listed incorporate a Cabibbo-Kobayashi-Maskawa- (CKM-) suppressed process excluding them from the semileptonic-type class. The theoretical analyses in the present work are general enough to allow for this special grouping, but for simplicity we disregard it in our Monte Carlo simulations. Incorporating it should result in some improvement over the bounds we obtain.

The analyses in the sections below involve transition amplitudes for the decay into a final state f, taken to be either a semileptonic-type state or a $J/\psi K^0$ (or conjugate) state. Following standard procedure, we disregard possible effects from penguin diagrams or other loop contributions and parametrize these amplitudes as [36–38]

$$\langle f|T|B^0\rangle = F_f(1 - y_f), \quad \langle f|T|\bar{B}^0\rangle = x_f F_f(1 - y_f),$$

$$\langle \bar{f}|T|\bar{B}^0\rangle = F_f^*(1 + y_f^*), \quad \langle \bar{f}|T|B^0\rangle = \bar{x}_f F_f^*(1 + y_f^*). \quad (4)$$

The independent complex quantities x_f, $\bar{x}_f$, F_f, and y_f are assumed small in what follows. Any possible violation of the $\Delta B = \Delta Q$ rule is parametrized by x_f and $\bar{x}_f$, both of which vanish if the rule is exact. Invariance under T implies x_f, $\bar{x}_f$, F_f, and y_f are real. Invariance under CPT implies $x_f = \bar{x}_f$ and $y_f = 0$. The quantity y_f parametrizes direct CPT violation in the decay to f.

Since the observed states are B_S and B_L, it is useful to obtain the associated transition amplitudes analogous to those in Eq. (4). Combining the definitions (1) and (4) and keeping only terms to first order in small quantities gives

$$\langle f|T|B_S\rangle = \frac{1}{\sqrt{2}}F_f(1 + \epsilon_B + \delta_B - y_f + x_f),$$

$$\langle f|T|B_L\rangle = \frac{1}{\sqrt{2}}F_f(1 + \epsilon_B - \delta_B - y_f - x_f),$$

$$\langle \bar{f}|T|B_S\rangle = \frac{1}{\sqrt{2}}F_f^*(1 - \epsilon_B - \delta_B + y_f^* + \bar{x}_f^*),$$

$$\langle \bar{f}|T|B_L\rangle = -\frac{1}{\sqrt{2}}F_f^*(1 - \epsilon_B + \delta_B + y_f^* - \bar{x}_f^*). \quad (5)$$

The theoretical analyses in the following sections incorporate the possibility of indirect T and CPT violation through the parameters ϵ_B and δ_B and allow for various sources of T and CPT violation through the parameters F_f, x_f, $\bar{x}_f$, and y_f. This level of generality has been kept for completeness. However, it is probable that some of these parameters are much smaller than others. For example, if CPT breaking does occur, general theoretical prejudice suggests that the magnitude of any indirect CPT violation is likely to be substantially larger than that of the direct CPT violation in any given channel. This is because δ_B is an

interferometric parameter, and moreover one that results from the combined effects over all channels of sources of *CPT* violation. These ideas are supported by analysis in the string scenario with spontaneously broken *CPT*, where quantities such as $\mathrm{Re}y_f$ are suppressed by many orders of magnitude relative to δ_B [10]. Note that in the standard purely phenomenological description the parameters $\mathrm{Re}\delta_B$ and $\mathrm{Im}\delta_B$ are undetermined and independent. In contrast, in the string scenario they are determined in terms of other quantities in the theory and are related through an additional constraint:

$$x \, \mathrm{Im}\delta_B \pm y \, \mathrm{Re}\delta_B = 0. \qquad (6)$$

For generality, we do *not* impose this condition in what follows.

A Monte Carlo simulation of a realistic experimental situation allowing for the full parameter range of all the available *T*- and *CPT*-violating parameters produces unwieldy results. For the illustrative purposes of the present work, we have therefore chosen to restrict the multiplicity of available variables as much as possible compatible with our goal of demonstrating the feasibility of extracting *CPT* bounds from realistic experimental data. In our simulations, we have taken advantage of the likely hierarchy in the magnitude of the various parameters, as described above, and have kept only quantities affecting indirect *T* and *CPT* violation. This restriction provides a meaningful approximation for extracting *CPT* bounds from experimental data.

As described in the Introduction, the present work contains Monte Carlo simulations of uncorrelated decays at a collider and of correlated decays at both symmetric and asymmetric *B* factories. We obtain four-vectors for *B* events from Z^0 decays and $\Upsilon(4S)$ decays using the JETSET 7.3 program [39] that models jet fragmentation, particle decays, and final-state parton showers. The full chain of detector simulation and event reconstruction is complex and unnecessary for our present purposes, so instead we statistically smear the four-vectors obtained from JETSET 7.3 according to the energy and momentum resolutions outlined for the OPAL detector [27], the CLEO II detector [28], and the BaBar detector [29]. Detector geometric acceptances are incorporated in all cases, as are typical reconstruction efficiencies estimated from existing publications or projected values. The possibility of measurement of various asymmetries as a function of proper decay time is considered, and typical resolutions of decay lengths and B^0-meson boosts are taken for each of the detectors mentioned. Additional details of the simulations are described in the relevant sections below.

III. UNCORRELATED SYSTEMS

A. Theory

This subsection provides the theoretical derivation of time-dependent and time-integrated amplitudes and rates for relevant decays of uncorrelated neutral *B* mesons.

We begin by considering decays into semileptonic-type final states *f*. Suppose an uncorrelated meson state $|B^0\rangle$ is produced at time $t=0$ and evolves to the state $|B(t)\rangle$ after a time *t* measured in the rest frame of the meson. The analo-

gous quantities for an antimeson are $|\bar{B}^0\rangle$ at $t=0$ and $|\bar{B}(t)\rangle$ at time *t*.

To obtain the time-dependent decay amplitudes, we proceed by inverting Eq. (1) to find the states $|B^0\rangle$ and $|\bar{B}^0\rangle$ and incorporating the time evolution via Eq. (2). Using Eq. (4), some algebra then leads to the following time-dependent decay probabilities:

$$P_f(t) \equiv |\langle f|T|B(t)\rangle|^2$$
$$= \tfrac{1}{4}|F_f|^2\{(1+4\,\mathrm{Re}\delta_B - 2\,\mathrm{Re}y_f + 2\,\mathrm{Re}x_f)\exp(-\gamma_S t)$$
$$+ (1-4\,\mathrm{Re}\delta_B - 2\,\mathrm{Re}y_f - 2\,\mathrm{Re}x_f)\exp(-\gamma_L t)$$
$$+ 2[(1-2\,\mathrm{Re}y_f)\cos\Delta mt$$
$$- (4\,\mathrm{Im}\delta_B + 2\,\mathrm{Im}x_f)\sin\Delta mt]\exp(-\gamma t/2)\},$$

$$\bar{P}_{\bar{f}}(t) \equiv |\langle\bar{f}|T|\bar{B}(t)\rangle|^2$$
$$= P_f(\delta_B \to -\delta_B, y_f \to -y_f, x_f \to \bar{x}_f^*),$$

$$P_{\bar{f}}(t) \equiv |\langle\bar{f}|T|B(t)\rangle|^2$$
$$= \tfrac{1}{4}|F_f|^2\{(1-4\,\mathrm{Re}\epsilon_B + 2\,\mathrm{Re}y_f + 2\,\mathrm{Re}\bar{x}_f)\exp(-\gamma_S t)$$
$$+ (1-4\,\mathrm{Re}\epsilon_B + 2\,\mathrm{Re}y_f - 2\,\mathrm{Re}\bar{x}_f)\exp(-\gamma_L t)$$
$$- 2[(1-4\,\mathrm{Re}\epsilon_B + 2\,\mathrm{Re}y_f)\cos\Delta mt$$
$$+ 2\,\mathrm{Im}\bar{x}_f\sin\Delta mt]\exp(-\gamma t/2)\},$$

$$\bar{P}_f(t) \equiv |\langle f|T|\bar{B}(t)\rangle|^2 = P_{\bar{f}}(\epsilon_B \to -\epsilon_B, y_f \to -y_f, \bar{x}_f \to x_f^*).$$
$$\qquad (7)$$

The decay probabilities $\bar{P}_{\bar{f}}$ and $\bar{P}_f$ are obtained by substituting as indicated in the expressions for P_f and $P_{\bar{f}}$. These probabilities are used in Sec. III B as input for our Monte Carlo simulations.

Intuition about the physical content of the decay probabilities can be obtained by considering the fully time-integrated rates and constructing various asymmetries. Explicitly, the time-integrated decay rates are

$$R_f \equiv \int_0^\infty dt P_f$$

$$= \tfrac{1}{4}|F_f|^2\left(\gamma\left[\frac{1}{\gamma_S\gamma_L} + \frac{1}{b^2}\right](1-2\,\mathrm{Re}y_f)\right.$$
$$\left. - \frac{2\Delta\gamma}{\gamma_S\gamma_L}(2\,\mathrm{Re}\delta_B + \mathrm{Re}x_f) - \frac{4\Delta m}{b^2}(2\,\mathrm{Im}\delta_B + \mathrm{Im}x_f)\right),$$

$$\bar{R}_{\bar{f}} \equiv \int_0^\infty dt \bar{P}_{\bar{f}}$$

$$= R_f(\delta_B \to -\delta_B, y_f \to -y_f, x_f \to \bar{x}_f^*),$$

$$R_{\bar f} \equiv \int_0^\infty dt\, P_{\bar f}$$

$$= \tfrac{1}{4}|F_f|^2 \Bigg(\gamma \left[\frac{1}{\gamma_S \gamma_L} - \frac{1}{b^2} \right](1 - 4\,\mathrm{Re}\epsilon_B + 2\,\mathrm{Re}y_f)$$

$$- \frac{2\Delta\gamma}{\gamma_S \gamma_L}\mathrm{Re}\bar{x}_f - \frac{4\Delta m}{b^2}\mathrm{Im}\bar{x}_f \Bigg),$$

$$\bar{R}_f \equiv \int_0^\infty dt\, \bar{P}_f$$

$$= R_{\bar f}(\epsilon_B \to -\epsilon_B, y_f \to -y_f, \bar{x}_f \to x_f^*). \qquad (8)$$

Two interesting independent asymmetries can be defined from these rates. One is

$$A_f \equiv \frac{R_f - \bar{R}_{\bar f}}{R_f + \bar{R}_{\bar f}}$$

$$= -2\,\mathrm{Re}y_f - \frac{1}{\gamma(b^2 + \gamma_S \gamma_L)}\{\Delta\gamma b^2[4\,\mathrm{Re}\delta_B + \mathrm{Re}(x_f - \bar{x}_f)]$$

$$+ 2\Delta m\,\gamma_S \gamma_L[4\,\mathrm{Im}\delta_B + \mathrm{Im}(x_f + \bar{x}_f)]\}. \qquad (9)$$

The other is

$$A'_f \equiv \frac{\bar{R}_f - R_{\bar f}}{\bar{R}_f + R_{\bar f}}$$

$$= 4\,\mathrm{Re}\epsilon_B - 2\,\mathrm{Re}y_f - \frac{1}{\gamma a^2}[\Delta\gamma b^2\,\mathrm{Re}(x_f - \bar{x}_f)$$

$$- 2\Delta m\,\gamma_S \gamma_L\,\mathrm{Im}(x_f + \bar{x}_f)]. \qquad (10)$$

These asymmetries provide insight about the information available from a complete analysis. As an example, in the case where y_f, x_f, and $\bar{x}_f$ are taken to be negligible, the first asymmetry gives information about indirect CPT violation while the second reduces to $A'_f = 4\,\mathrm{Re}\epsilon_B$.

We next consider decays into the final states of the form $J/\psi K$, which lie outside the semileptonic-type class. The physical final states involve the linear combinations K_S and K_L given by the kaon equivalent of Eq. (1). They are denoted by $\langle J/\psi K_S|$ and $\langle J/\psi K_L|$.

The four possible time-dependent decay probabilities,

$$P_S(t) \equiv |\langle J/\psi K_S|T|B(t)\rangle|^2$$

$$= (\mathrm{Re}F_{J/\psi})^2 \Bigg(\left[\tfrac{1}{2} - \mathrm{Re}\epsilon_B + \mathrm{Re}\delta_B + \tfrac{1}{2}(\mathrm{Re}x_{J/\psi} + \mathrm{Re}\bar{x}_{J/\psi}) \right]\exp(-\gamma_S t)$$

$$+ \Bigg\{ \left[\mathrm{Re}\epsilon_K + \mathrm{Re}\epsilon_B + \mathrm{Re}\delta_K - \mathrm{Re}\delta_B - \mathrm{Re}y_{J/\psi} - \tfrac{1}{2}\mathrm{Re}(x_{J/\psi} - \bar{x}_{J/\psi}) \right]\cos\Delta mt$$

$$- \left[\mathrm{Im}\epsilon_K - \mathrm{Im}\epsilon_B + \mathrm{Im}\delta_K + \mathrm{Im}\delta_B + \tfrac{1}{2}\mathrm{Im}(x_{J/\psi} + \bar{x}_{J/\psi}) - \frac{\mathrm{Im}F_{J/\psi}}{\mathrm{Re}F_{J/\psi}} \right]\sin\Delta mt \Bigg\}\exp(-\gamma t/2) \Bigg),$$

$$\bar{P}_S(t) \equiv |\langle J/\psi K_S|T|\bar{B}(t)\rangle|^2$$

$$= P_S(\epsilon_K \to -\epsilon_K, \epsilon_B \to -\epsilon_B, \delta_K \to -\delta_K, \delta_B \to -\delta_B, y_{J/\psi} \to -y_{J/\psi}, x_{J/\psi} \leftrightarrow \bar{x}_{J/\psi}^*, F_{J/\psi} \to F_{J/\psi}^*),$$

$$P_L(t) \equiv |\langle J/\psi K_L|T|B(t)\rangle|^2$$

$$= (\mathrm{Re}F_{J/\psi})^2 \Bigg\{ \left[\tfrac{1}{2} - \mathrm{Re}\epsilon_B - \mathrm{Re}\delta_B - \tfrac{1}{2}(\mathrm{Re}x_{J/\psi} + \mathrm{Re}\bar{x}_{J/\psi}) \right]\exp(-\gamma_L t)$$

$$+ \Bigg\{ \left[\mathrm{Re}\epsilon_K + \mathrm{Re}\epsilon_B - \mathrm{Re}\delta_K + \mathrm{Re}\delta_B - \mathrm{Re}y_{J/\psi} + \tfrac{1}{2}\mathrm{Re}(x_{J/\psi} - \bar{x}_{J/\psi}) \right]\cos\Delta mt$$

$$+ \left[\mathrm{Im}\epsilon_K - \mathrm{Im}\epsilon_B - \mathrm{Im}\delta_K - \mathrm{Im}\delta_B - \tfrac{1}{2}\mathrm{Im}(x_{J/\psi} + \bar{x}_{J/\psi}) - \frac{\mathrm{Im}F_{J/\psi}}{\mathrm{Re}F_{J/\psi}} \right]\sin\Delta mt \Bigg\}\exp(-\gamma t/2) \Bigg),$$

$$\bar{P}_L(t) \equiv |\langle J/\psi K_L|T|\bar{B}(t)\rangle|^2$$

$$= P_L(\epsilon_K \to -\epsilon_K, \epsilon_B \to -\epsilon_B, \delta_K \to -\delta_K, \delta_B \to -\delta_B, y_{J/\psi} \to -y_{J/\psi}, x_{J/\psi} \leftrightarrow \bar{x}_{J/\psi}^*, F_{J/\psi} \to F_{J/\psi}^*), \qquad (11)$$

can be found by a procedure analogous to that yielding Eq. (7). The above expressions for P_S and $\bar{P}_S$ are used as input to our Monte Carlo simulations in Sec. III B.

As in the semileptonic-type case, insight can be obtained from the fully integrated rates. The four time-integrated rates corresponding to the above decay probabilities are

$$R_S = \int_0^\infty dt\, P_S$$

$$= (\mathrm{Re}F_{J/\psi})^2 \left(\frac{1}{2\gamma_S} - \left[\frac{1}{\gamma_S} - \frac{\gamma}{2b^2} \right] (\mathrm{Re}\epsilon_B - \mathrm{Re}\delta_B - \tfrac{1}{2}\,\mathrm{Re}x_{J/\psi}) + \tfrac{1}{2}\left[\frac{1}{\gamma_S} + \frac{\gamma}{2b^2} \right] \mathrm{Re}\overline{x}_{J/\psi} + \frac{\gamma}{2b^2}(\mathrm{Re}\epsilon_K + \mathrm{Re}\delta_K - \mathrm{Re}y_{J/\psi}) \right.$$

$$\left. - \frac{\Delta m}{b^2}\left[\mathrm{Im}\epsilon_K - \mathrm{Im}\epsilon_B + \mathrm{Im}\delta_K + \mathrm{Im}\delta_B + \tfrac{1}{2}\,\mathrm{Im}(x_{J/\psi} + \overline{x}_{J/\psi}) - \frac{\mathrm{Im}F_{J/\psi}}{\mathrm{Re}F_{J/\psi}} \right] \right),$$

$$\overline{R}_S = \int_0^\infty dt\, \overline{P}_S$$

$$= R_S(\epsilon_K \to -\epsilon_K, \epsilon_B \to -\epsilon_B, \delta_K \to -\delta_K, \delta_B \to -\delta_B, y_{J/\psi} \to -y_{J/\psi}, x_{J/\psi} \leftrightarrow \overline{x}^*_{J/\psi}, F_{J/\psi} \to F^*_{J/\psi}),$$

$$R_L = \int_0^\infty dt\, P_L$$

$$= (\mathrm{Re}F_{J/\psi})^2 \left(\frac{1}{2\gamma_L} - \left[\frac{1}{\gamma_L} - \frac{\gamma}{2b^2} \right] (\mathrm{Re}\epsilon_B + \mathrm{Re}\delta_B + \tfrac{1}{2}\,\mathrm{Re}x_{J/\psi}) - \tfrac{1}{2}\left[\frac{1}{\gamma_L} + \frac{\gamma}{2b^2} \right] \mathrm{Re}\overline{x}_{J/\psi} + \frac{\gamma}{2b^2}(\mathrm{Re}\epsilon_K - \mathrm{Re}\delta_K - \mathrm{Re}y_{J/\psi}) \right.$$

$$\left. + \frac{\Delta m}{b^2}\left[\mathrm{Im}\epsilon_K - \mathrm{Im}\epsilon_B - \mathrm{Im}\delta_K - \mathrm{Im}\delta_B - \tfrac{1}{2}\,\mathrm{Im}(x_{J/\psi} + \overline{x}_{J/\psi}) - \frac{\mathrm{Im}F_{J/\psi}}{\mathrm{Re}F_{J/\psi}} \right] \right),$$

$$\overline{R}_L = \int_0^\infty dt\, \overline{P}_L$$

$$= R_L(\epsilon_K \to -\epsilon_K, \epsilon_B \to -\epsilon_B, \delta_K \to -\delta_K, \delta_B \to -\delta_B, y_{J/\psi} \to -y_{J/\psi}, x_{J/\psi} \leftrightarrow \overline{x}^*_{J/\psi}, F_{J/\psi} \to F^*_{J/\psi}). \tag{12}$$

The replacements indicated by a double-headed arrow involve parameter interchange rather than substitution.

Two theoretically interesting asymmetries can be constructed from the above decay rates. One is

$$A_S \equiv \frac{\overline{R}_S - R_S}{\overline{R}_S + R_S}$$

$$= 2\left(1 - \frac{\gamma\gamma_S}{2b^2} \right) \mathrm{Re}(\epsilon_B - \delta_B) + \frac{\gamma\gamma_S}{2b^2}\,\mathrm{Re}(x_{J/\psi} - \overline{x}_{J/\psi}) - \frac{\gamma\gamma_S}{b^2}\,\mathrm{Re}(\epsilon_K + \delta_K - y_{J/\psi})$$

$$+ \frac{2\Delta m\,\gamma_S}{b^2}\left(\mathrm{Im}\epsilon_K - \mathrm{Im}\epsilon_B + \mathrm{Im}\delta_K + \mathrm{Im}\delta_B + \tfrac{1}{2}\,\mathrm{Im}(x_{J/\psi} + \overline{x}_{J/\psi}) - \frac{\mathrm{Im}F_{J/\psi}}{\mathrm{Re}F_{J/\psi}} \right). \tag{13}$$

The other is the analogous quantity for the decays involving K_L:

$$A_L \equiv \frac{\overline{R}_L - R_L}{\overline{R}_L + R_L}$$

$$= A_S(\gamma_S \leftrightarrow \gamma_L, \epsilon_K \to \epsilon^*_K, \epsilon_B \to \epsilon^*_B, \delta_K \to -\delta^*_K, \delta_B \to -\delta^*_B, x_{J/\psi} \to -x^*_{J/\psi}, \overline{x}_{J/\psi} \to -\overline{x}^*_{J/\psi}, F_{J/\psi} \to F^*_{J/\psi}). \tag{14}$$

Of these two asymmetries, only the one involving K_S is considered because detection of the K_L is difficult with current experimental techniques.

B. Experiment

In this subsection, we describe the results of a Monte Carlo simulation involving uncorrelated *B* decays observed by a typical detector at a high-energy collider. For definiteness, we use a detector simulation that smears four-vectors according to the resolutions for charged-track and neutral-energy measurements of the OPAL detector [27] at LEP.

The JETSET 7.3 [39] event generator is used to simulate both B_d^0 signal events and background events from Z^0 decays into light-quark pairs and into other *B* hadrons. As discussed in Sec. II, we restrict the variables in our simulation to parameters controlling indirect *T* and indirect *CPT* violation. This simplifies many of the relevant equations in the previous subsection. The time-dependent mixing probabilities for the signal are sampled from the probability distributions given for $B^0 \to D^{(*)}\ell\nu$ decays in Eq. (7) and for $B^0 \to J/\psi K_S$ in Eq. (11). The decay length L is found from the magnitude p_B of the generated momentum of the signal B^0 meson.

For $B^0 \to D^{(*)}\ell\nu$ decays, a typical decay-length resolution $\sigma_L = 200$ μm is taken [40]. We assume the boost of the B^0 could be estimated with techniques using scaled $D\ell$ momenta, producing a resultant fractional resolution $\sigma_{p_B}/p_B = 0.11$ [41]. Rather than reconstructing vertices with the smeared four-vectors, the reconstructed proper time t is simply smeared according to

$$\left(\frac{\sigma_t}{t}\right)^2 = \left(\frac{\sigma_L}{L}\right)^2 + \left(\frac{\sigma_{p_B}}{p_B}\right)^2. \tag{15}$$

For the fully exclusive $B^0 \to J/\psi K_S$ decay, an estimated decay-length resolution of $\sigma_L = 300$ μm is used. The smeared decay length is first found, and the momentum reconstructed from the sum of the smeared four-vectors of the decay products is subsequently used to determine the proper decay time.

We first discuss in detail our analysis of semileptonic decays. In this case, a useful quantity for CPT studies is the time-dependent asymmetry of decay probabilities given by

$$A(f,t) \equiv \frac{\bar{P}_{\bar{f}}(t) - P_f(t)}{\bar{P}_{\bar{f}}(t) + P_f(t)}$$

$$\approx 4 \, \mathrm{Im}\delta_B \frac{\sin\Delta mt}{(1 + \cos\Delta mt)}. \tag{16}$$

In deriving this result, we have neglected direct CPT and $\Delta B = \Delta Q$ violations and have approximated $\gamma_S \simeq \gamma_L$. The latter implies that $\Delta\gamma$ can be treated as small over the range of time scales considered.

Another key quantity is the difference of time-dependent asymmetries of decay probabilities, given by

$$D(f,t) \equiv \frac{\bar{P}_{\bar{f}}(t) - \bar{P}_f(t)}{\bar{P}_{\bar{f}}(t) + \bar{P}_f(t)} - \frac{P_f(t) - P_{\bar{f}}(t)}{P_f(t) + P_{\bar{f}}(t)}$$

$$\approx -4 \, \mathrm{Re}\epsilon_B(1 - \cos\Delta mt) + 4 \, \mathrm{Im}\delta_B\sin\Delta mt, \tag{17}$$

where the same approximations have been made.

To construct these asymmetries experimentally, the b flavor of the B meson at both the decay and the production times must be determined. The flavor at the decay time is tagged by the charge of the lepton. The flavor at the production time can be identified using a jet-charge technique [41]. It is assumed that this method is incorrect 20% of the time [41,42]. This mistag probability, the proper time resolution discussed above, and the backgrounds to the signal all dilute the magnitude of the experimentally observed asymmetry.

The expected levels of various backgrounds are estimated from previous experimental measurements of Δm_d [41,42]. Approximately 20% of the selected sample can be expected to be combinatorial background without lifetime information, arising from the primary vertex of the event. This fraction of events is folded in with a distribution in the proper decay time consistent with a Gaussian distribution of width σ_t. About another 10% of the selected sample is expected to arise from other genuine B-hadron decays with lifetime information that are misidentified as $B^0 \to D^{(*)}\ell\nu$. The decay-
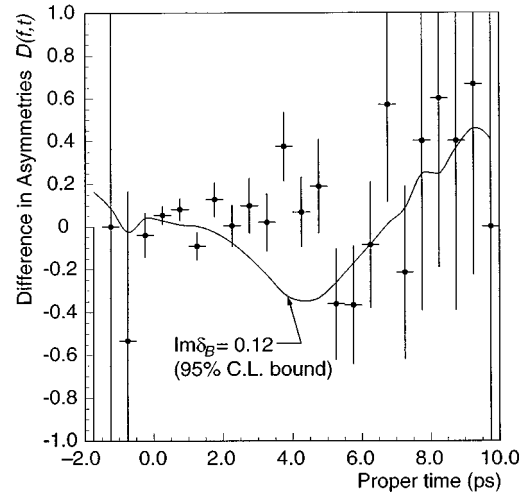

FIG. 1. Simulated data and bound for the uncorrelated case in the semileptonic channel. The points with error bars represent the typical observed difference of asymmetries $D(f,t)$ as a function of time for 1500 $B^0 \to D^{(*)}\ell\nu$ decays generated in a Monte Carlo simulation with $\mathrm{Im}\delta_B = 0$. Superimposed as a solid line is the predicted shape of $D(f,t)$ for $\mathrm{Im}\delta_B = 0.12$, which for this sample is the upper bound at the 95% C.L. determined from the difference of likelihood in binned likelihood fits.

time distribution of these events is taken to be an exponential consistent with the average B-hadron lifetime [30] convoluted with a Gaussian of width σ_t, but without the mixing time dependence of Eq. (7).

For a perfect detector and with the approximations we have made, the form of Eq. (16) contains a pole structure at $\cos\Delta mt = -1$. The observed magnitude of this asymmetry would be sensitive to the precise knowledge of the detector resolution, mistag probabilities, and backgrounds. We therefore focus instead on the difference of asymmetries given in Eq. (17) as an experimental observable for the semileptonic case.

To test the prospect for measuring or bounding $\mathrm{Im}\delta_B$ via semileptonic decays, we generated large Monte Carlo samples of 10^6 events each that included all the above effects for a range of values of $\mathrm{Im}\delta_B$. For definiteness in this and all other analyses described below [43], we set ϵ_B to the value [44] $\epsilon_B = 0.045$. For each sample, the difference in asymmetries of Eq. (17) was constructed.

For $\mathrm{Im}\delta_B = 0$, we then generated an ensemble of 200 datasets of Monte Carlo events. Each such dataset contained 1500 $B^0 \to D^{(*)}\ell\nu$ decays, a statistical sample that could possibly be reconstructed by combining the present data from all the LEP Collaborations. For the observed $D(f,t)$ distribution in each of these simulated datasets, we performed binned maximum-likelihood fits to the expected shape for a particular value of $\mathrm{Im}\delta_B$. This determined the average bound that could be set on $\mathrm{Im}\delta_B$. Subsequently, we repeated the same process for dataset ensembles with $\mathrm{Im}\delta_B = 0.1$ and $\mathrm{Im}\delta_B = 0.2$.

From the ensemble of 200 datasets for the semileptonic case that were generated using $\mathrm{Im}\delta_B = 0$, the average value of the 95%-confidence-level (C.L.) upper bound on $\mathrm{Im}\delta_B$ that can be placed on a single dataset is $\mathrm{Im}\delta_B < 0.12$. Figure 1 shows the result from a typical dataset that gives rise to
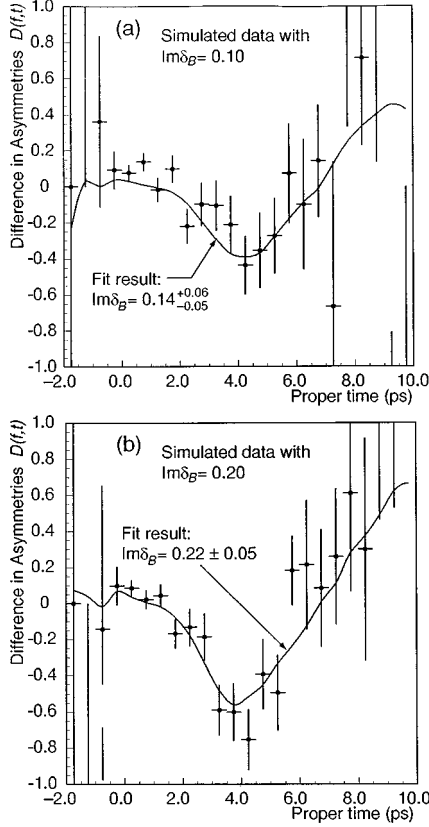
FIG. 2. Simulated data and fits for the uncorrelated case in the semileptonic channel for (a) $\mathrm{Im}\delta_B=0.1$, (b) $\mathrm{Im}\delta_B=0.2$. In each plot, the points with error bars represent the typical observed difference of asymmetries $D(f,t)$ as a function of time for 1500 $B^0 \rightarrow D^{(*)}\ell\nu$ decays generated in a Monte Carlo simulation with the indicated value of $\mathrm{Im}\delta_B$. Superimposed as solid lines are the predicted shapes of $D(f,t)$ found from binned likelihood fits. The fit results and associated precisions are also indicated.
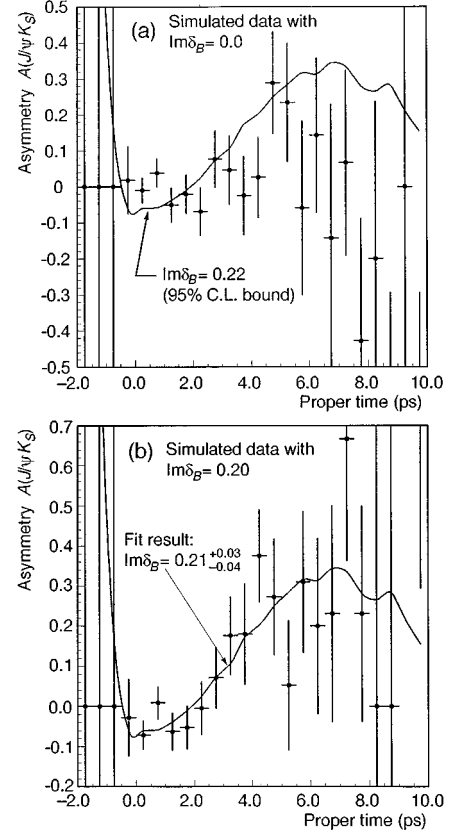
FIG. 3. Simulated data for the uncorrelated case in the $J/\psi K_S$ channel. (a) The points with error bars represent the typical observed asymmetry $A(J/\psi K_S)$ as a function of time for 500 $B^0 \rightarrow J/\psi K_S$ decays generated in a Monte Carlo simulation with $\mathrm{Im}\delta_B=0$. Superimposed as a solid line is the predicted shape for $\mathrm{Im}\delta_B=0.22$, which for this sample is the upper bound at the 95% C.L. determined from the difference of likelihood in binned likelihood fits. (b) Same as in (a) but for 1500 $B^0 \rightarrow J/\psi K_S$ decays generated in a Monte Carlo simulation with $\mathrm{Im}\delta_B=0.2$. The solid line is the predicted shape. The fit result and associated precisions are also indicated.

this limit. For the dataset illustrated, the probability is 25% that the data are from a parent distribution with $\mathrm{Im}\delta_B=0$.

Assuming indirect *CPT* violation indeed exists, Fig. 2 shows typical fits and precisions to simulated data generated with $\mathrm{Im}\delta_B=0.10$ and $\mathrm{Im}\delta_B=0.20$. In the samples indicated, the probabilities that the simulated datasets are from parent distributions with $\mathrm{Im}\delta_B=0$ are 0.5% and 0.1%, respectively.

We next turn to an investigation of decays into $J/\psi K_S$. In this case, a useful quantity is the time-dependent asymmetry of decay probabilities given by

$$
A(J/\psi K_S, t) \equiv \frac{\overline{P}_S(t) - P_S(t)}{\overline{P}_S(t) + P_S(t)}
$$

$$
\approx 2\ \mathrm{Re}\epsilon_B - 2\ \mathrm{Re}\delta_B
$$

$$
-2(\ \mathrm{Re}\epsilon_K + \ \mathrm{Re}\epsilon_B + \ \mathrm{Re}\delta_K - \ \mathrm{Re}\delta_B)\cos\Delta mt
$$

$$
+2(\ \mathrm{Im}\epsilon_K - \ \mathrm{Im}\epsilon_B + \ \mathrm{Im}\delta_K + \ \mathrm{Im}\delta_B)\sin\Delta mt.
$$

$$
(18)
$$

In deriving this expression, approximations similar to those in Eq. (16) have been made. If $\mathrm{Re}\delta_B$ and $\mathrm{Im}\delta_B$ are to be bounded at levels greater than known limits on the other parameters, then this expression effectively reduces to

$$
A(J/\psi K_S, t) \approx -2\ \mathrm{Re}\delta_B(1-\cos\Delta mt) + 2\ \mathrm{Im}\delta_B\sin\Delta mt.
$$

$$
(19)
$$

We find that the small branching ratio for the hadronic decay $B^0 \rightarrow J/\psi K_S$ and the relatively small reconstruction efficiency make it unlikely that current LEP data can bound *CPT* effects in this channel. As an example, ALEPH has a sample of only four events of this type among the 3×10^6 Z^0 decays used to measure the B^0 lifetime [45]. Samples of $B^0 \rightarrow J/\psi K_S$ in uncorrelated B^0 events collected by the Collider Detector at Fermilab (CDF) Collaboration at the Tevatron are larger, but still insufficient. However, there are more

promising prospects for larger samples in approximately 1 fb^{-1} of data to be obtained after the Fermilab main injector [46] begins operation.

For illustrative purposes and using the asymmetry of Eq. (19) as the experimental observable with $\epsilon_B = 0.045$ as before, Fig. 3(a) shows the bound that could be placed on $\mathrm{Im}\delta_B$ from samples of 500 reconstructed $B^0 \rightarrow J/\psi K_S$ decays including resolutions outlined previously. The background levels are much smaller since this channel is particularly clean. Even with these large samples, the limits at the 95% C.L. are $\mathrm{Im}\delta_B < 0.22$. Figure 3(b) shows the feasibility for a typical measurement of indirect CPT violation, assuming an even larger sample of 1500 reconstructed $J/\psi K_S$ decays.

IV. CORRELATED SYSTEMS

A. Theory

In this subsection, we summarize some key formulas for the situation where correlated pairs of neutral B mesons are produced. Since our Monte Carlo simulations neglect effects other than from indirect T and CPT violation, and since the general analysis is already available in the literature [10,19], we restrict ourselves here to consideration only of those asymmetries directly useful for the simulations. A more complete theoretical analysis is given in Refs. [10,19], where the reader can also find additional details of some of the derivations below. For simplicity in what follows, we take the correlated mesons as B_d-$\bar{B}_d$ pairs formed from the decay of the $\Upsilon(4S)$. Much of the discussion can be extended to the case of B_s pairs, along the lines suggested in Ref. [10].

We work in the rest frame of the $\Upsilon(4S)$ resonance, choosing to align the z-coordinate axis with the momenta of the B pair. Since the $\Upsilon(4S)$ has $J^{PC} = 1^{--}$, the initial state $|i\rangle$ of the B-meson pair immediately following the decay is

$$|i\rangle = \frac{1}{\sqrt{2}}[|B_S(\hat{z})B_L(-\hat{z})\rangle - |B_L(\hat{z})B_S(-\hat{z})\rangle], \quad (20)$$

where the argument $(\pm\hat{z})$ indicates the direction of the momentum. To simplify notation, we label the two mesons by an index $\alpha = 1,2$ and suppose they decay at times t_α into final states $|f_\alpha\rangle$.

The amplitude $\mathcal{A}_{12}(t_1,t_2)$ for the decay can be written in terms of the transition amplitudes $a_{\alpha S} = \langle f_\alpha|T|B_S\rangle$, $a_{\alpha L} = \langle f_\alpha|T|B_L\rangle$ and their ratios $\eta_\alpha = a_{\alpha L}/a_{\alpha S}$. The result is

$$\mathcal{A}_{12}(t_1,t_2)$$
$$= \frac{1}{\sqrt{2}}a_{1S}a_{2S}(\eta_2\exp[-i(m_St_1+m_Lt_2)-\tfrac{1}{2}(\gamma_St_1+\gamma_Lt_2)]$$
$$- \eta_1\exp[-i(m_Lt_1+m_St_2)-\tfrac{1}{2}(\gamma_Lt_1+\gamma_St_2)]). \quad (21)$$

This expression is the basic input for the Monte Carlo simulations in the next two subsections.

The presence of two time variables implies the existence of several types of time integrated rates. One useful case is obtained by integration over the linear combination

$$t = t_1 + t_2. \quad (22)$$

This produces a rate dependent only on the time difference, which reduces some experimental systematics. Thus, integrating over t with Δt fixed yields the once-integrated rate

$$I(f_1,f_2,\Delta t) = \tfrac{1}{2}\int_{|\Delta t|}^{\infty} dt|\mathcal{A}_{12}(t_1,t_2)|^2$$

$$= \frac{|a_{1L}a_{2S}|^2}{2\gamma}e^{-\gamma|\Delta t|/2}[e^{-\Delta\gamma\Delta t/2}+|r_{21}|^2e^{\Delta\gamma\Delta t/2}$$

$$- 2\,\mathrm{Re}r_{21}\cos\Delta m\Delta t - 2\,\mathrm{Im}r_{21}\sin\Delta m\Delta t], \quad (23)$$

where $r_{21} = \eta_2/\eta_1$.

Other useful once-integrated rates are produced by integrating over the orthogonal linear combination

$$\Delta t = t_2 - t_1 \quad (24)$$

with t held fixed. The natural possibilities are

$$J(f_1,f_2,t) = \tfrac{1}{2}\int_{-t}^{t} d\Delta t|\mathcal{A}_{12}(t_1,t_2)|^2$$

$$= \tfrac{1}{2}|a_{1L}a_{2S}|^2e^{-\gamma t/2}\left[\frac{1}{\Delta\gamma}(1+|r_{21}|^2)\right.$$

$$\left.\times(e^{\Delta\gamma t/2}-e^{-\Delta\gamma t/2}) - \frac{2\,\mathrm{Re}r_{21}}{\Delta m}\sin\Delta mt\right], \quad (25)$$

$$J^+(f_1,f_2,t) = \tfrac{1}{2}\int_0^t d\Delta t|\mathcal{A}_{12}(t_1,t_2)|^2$$

$$= \tfrac{1}{2}|a_{1L}a_{2S}|^2e^{-\gamma t/2}\left[\frac{1}{\Delta\gamma}(1-e^{-\Delta\gamma t/2}-|r_{21}|^2\right.$$

$$+ |r_{21}|^2e^{\Delta\gamma t/2}) - \frac{1}{\Delta m}[\,\mathrm{Re}r_{21}\sin\Delta mt$$

$$\left.+ \mathrm{Im}r_{21}(1-\cos\Delta mt)]\right], \quad (26)$$

$$J^-(f_1,f_2,t) = \tfrac{1}{2}\int_{-t}^{0} d\Delta t|\mathcal{A}_{12}(t_1,t_2)|^2$$

$$= -e^{-\gamma t}J^+(f_1,f_2,-t). \quad (27)$$

These two once-integrated rates are used for the simulations in the next two subsections.

Integration over the remaining variable to produce twice-integrated rates independent of the times t_1 and t_2 can be performed with several different integration limits. If the range is complete, this procedure produces the fully time-integrated rate $\Gamma(f_1,f_2)$ for the double-meson decay into final states f_1 and f_2. However, it is useful to introduce also the partial rates $\Gamma^+(f_1,f_2)$ for which the decay into f_1 occurs first and $\Gamma^-(f_1,f_2)$ for which it occurs second. This yields the expressions

$$\Gamma(f_1,f_2) = \int_{-\infty}^{\infty} d\Delta t \ I(f_1,f_2,\Delta t)$$

$$= \frac{1}{2\gamma_S\gamma_L}\left[|a_{1S}a_{2L}|^2 + |a_{1L}a_{2S}|^2 - \frac{\gamma_S\gamma_L}{b^2}\right.$$

$$\left. \times(a_{1S}^*a_{2L}^*a_{1L}a_{2S}+\text{c.c.})\right],$$

$$\Gamma^+(f_1,f_2) = \int_0^{\infty} d\Delta t \ I(f_1,f_2,\Delta t)$$

$$= \frac{1}{2\gamma}\left[\frac{|a_{1S}a_{2L}|^2}{\gamma_L} + \frac{|a_{1L}a_{2S}|^2}{\gamma_S}\right.$$

$$\left. -\left(\frac{a_{1S}^*a_{2L}^*a_{1L}a_{2S}}{\frac{1}{2}\gamma-i\Delta m}+\text{c.c.}\right)\right],$$

$$\Gamma^-(f_1,f_2) = \int_{-\infty}^{0} d\Delta t \ I(f_1,f_2,\Delta t)$$

$$= \Gamma^+(f_1,f_2)|_{m_S\leftrightarrow m_L, \gamma_S\leftrightarrow\gamma_L}. \tag{28}$$

Given these integrated rates, we can form asymmetries containing the essential information. An asymmetry useful for extracting the *T*-violation parameter $\text{Re}\epsilon_B$ is

$$A_{f,\bar{f}}^{\text{tot}} \equiv \frac{\Gamma(f,f)-\Gamma(\bar{f},\bar{f})}{\Gamma(f,f)+\Gamma(\bar{f},\bar{f})} = 4 \ \text{Re}(\epsilon_B - y_f). \tag{29}$$

We remark in passing that the incorporation of inclusive rates permits the extraction of the *T*-violation parameter $\text{Re}\epsilon_B$ independently of $\text{Re}y_f$ [19].

To obtain the real part of δ_B, which parametrizes indirect *CPT* violation, it is useful to consider double-meson decays into a semileptonic-type state f in one channel and into $J/\psi K_S$ in the second. We disregard decays into $J/\psi K_L$ in what follows because they are difficult to observe experimentally. The relevant ratio of matrix elements is

$$\eta_{J/\psi K_S} \equiv \frac{\langle J/\psi K_S|T|B_L\rangle}{\langle J/\psi K_S|T|B_S\rangle}$$

$$= \epsilon_K^* + \epsilon_B + \delta_K^* - \delta_B - \text{Re}y_{J/\psi}$$

$$-\frac{1}{2}(x_{J/\psi}-\bar{x}_{J/\psi}^*) + i\frac{\text{Im}F_{J/\psi}}{\text{Re}F_{J/\psi}}. \tag{30}$$

Here, the quantities ϵ_K and δ_K are measures of indirect *T* and *CPT* violation in the kaon system, analogous to ϵ_B and δ_B in the *B* system. We have assumed that $\text{Im}F_{J/\psi}$ is a small quantity, which is reasonable since it governs direct *T* violation. This ratio of matrix elements enters the rate asymmetry useful for the extraction of the real part of δ_B, which is

$$A_{f,K_S} \equiv \frac{\Gamma(f,J/\psi K_S)-\Gamma(\bar{f},J/\psi K_S)}{\Gamma(f,J/\psi K_S)+\Gamma(\bar{f},J/\psi K_S)}$$

$$= 2 \ \text{Re}(\epsilon_B - y_f - \delta_B) - \frac{2\gamma_S\gamma_L}{b^2} \ \text{Re}\eta_{J/\psi K_S}. \tag{31}$$

The above formula assumes that $x_f=\bar{x}_f$ and $x_{J/\psi}=\bar{x}_{J/\psi}$, i.e., that violations of the $\Delta B=\Delta Q$ rule are independent of violations of *CPT* invariance. The kaon-system parameters and ϵ_B are of order 10^{-3} or less, so this latter asymmetry provides a means of limiting or measuring $\text{Re}\delta_B$ at levels larger than this, under the assumption of negligible direct *CPT* violation.

Once $\text{Re}\delta_B$ is known, the extraction of the imaginary part of δ_B can be performed using another asymmetry involving double-semileptonic decay, given by

$$A_{f,\bar{f}} \equiv \frac{\Gamma^+(f,\bar{f})-\Gamma^-(f,\bar{f})}{\Gamma^+(f,\bar{f})+\Gamma^-(f,\bar{f})}$$

$$= 4\frac{b^2\Delta\gamma \ \text{Re}\delta_B + 2\Delta m \ \gamma_S\gamma_L \ \text{Im}\delta_B}{\gamma(b^2+\gamma_S\gamma_L)}. \tag{32}$$

In this case, the derivation assumes $x_f=\bar{x}_f^*$ i.e., that any violation of $\Delta B=\Delta Q$ is independent of *CP* violation.

B. Experiment: Unboosted case

In this subsection, we describe the results of a Monte Carlo simulation involving correlated *B* decays observed by a detector at a symmetric *B* factory, where the energies of the colliding electron and positron beams are equal. For definiteness, we use a detector simulation equivalent to the performance of the upgraded CLEO experiment at CESR, for which luminosity upgrades should allow the collection of large samples of data comparable in size and rate to those accumulated by the *B* factories at SLAC and KEK.

Four-vectors are smeared as described in the previous section, except that we use appropriate resolutions for charged-track and neutral-energy measurements for the CLEO II detector [28]. A decay-length resolution of $\sigma_L=150 \ \mu$m is taken for the reconstruction of vertices from both $B^0\rightarrow D^{(*)}\ell\nu$ decays and $B^0\rightarrow J/\psi K_S$ decays. Difficulties with the time resolution can immediately be anticipated since the B^0 mesons are produced almost at rest, which leads to short average decay lengths. Simulations confirm that measuring the time dependence of the decay-time asymmetries is infeasible using either the CLEO II detector or even the future CLEO III [47] detector. Indeed, the planned silicon-microvertex detectors for CLEO will primarily be used for background rejection rather than for the measurement of lifetimes.

Despite these difficulties, total-rate asymmetries can still be considered. Note, for example, that the *T*-violation parameter ϵ_B can be measured using the asymmetry of Eq. (29). More relevant for our present purposes is that the time-integrated asymmetry presented in Eq. (31) can be used at a symmetric *B* factory to extract $\text{Re}\delta_B$.

For our simulations, we take typical CLEO reconstruction efficiencies and backgrounds for the decay $B^0\rightarrow D^{(*)}\ell\nu$ (see Refs. [48]) and $B^0\rightarrow J/\psi K_S$ (see Ref. [49]). With an integrated luminosity of 100 fb^{-1} equivalent to about 54 million correlated B^0-$\bar{B}^0$ events, we estimate that reconstruction is possible for approximately 3200 signal events in which one B^0 meson decays into $D^{(*)}\ell\nu$ while the other decays into $J/\psi K_S$. The sign of the electric charge of the

lepton in the semileptonic decay can be used to determine whether an f or $\bar{f}$ state is present.

As discussed in Sec. II, we restrict the variables in our simulation to parameters controlling indirect T and indirect CPT violation. Taking $\epsilon_B = 0.045$ as before, the asymmetry of Eq. (31) can be used to set an estimated limit of $\mathrm{Re}\,\delta_B < 0.03$ at the 95% C.L. Present integrated luminosities at CLEO of about 2.0 fb^{-1} would give weak bounds of $\mathrm{Re}\,\delta_B \lesssim 0.35$.

C. Experiment: Boosted case

More confidence in the limits on or measurements of δ_B obtained through its effects on the observed time evolution of the correlated B system can be obtained in asymmetric machines presently under construction. The planned B factories at SLAC and KEK will collide e^+ and e^- at different energies. The result is a moving $\Upsilon(4S)$ that subsequently decays into $B^0 \bar{B}^0$. Each B^0 then eventually decays, producing a secondary vertex that can be reconstructed.

Since both B mesons are boosted along the beam direction and have little transverse momentum, the difference in decay points is primarily along the beam or $\hat{z}$ direction. For a 9 GeV e^- beam colliding with a 3.1 GeV e^+ beam as being planned for the B factory at SLAC, the average separation in z between the two decay vertices is approximately 200 μm. With a sufficiently sophisticated vertex detector, precisions can be attained allowing the measurement of the time evolution of the B^0-$\bar{B}^0$ system. The goal of the B factory is to measure the time-dependent asymmetry in decays to CP eigenstates, but the effects of CPT violation can also be elucidated.

Here, we describe the results of a Monte Carlo simulation involving correlated B decays observed by a representative detector at a typical asymmetric B factory. For definiteness, we use a detector simulation approximating the future BaBar detector [29] at SLAC. With minor changes, our results should also be valid for the BELLE experiment at KEK. As before, we restrict the variables in our simulation to parameters controlling indirect T and indirect CPT violation.

We again employ smeared four-vectors for these simulations. The correlated decay times t_1 and t_2 are sampled according to the relations given in Eqs. (21), (23), and (25). From the generated momentum of each signal B^0 meson, two decay lengths L_1 and L_2 are found. We assume a typical decay-length resolution of $\sigma_L = 60 \ \mu$m [29]. The proper decay times t_1 and t_2 are then extracted for the B_S and $\bar{B}_L$ decays via the experimentally accessible channels $B^0 \to D^{(*)} \ell \nu$ and/or $B^0 \to J/\psi K_S$, using the techniques described in Sec. III B.

We consider first the case where both B mesons decay semileptonically into $D^{(*)} \ell \nu$. The following two useful t- or Δt-dependent asymmetries of once-integrated decay probabilities can be obtained:

$$A(f,\bar{f},\Delta t) \equiv \frac{I(f,\bar{f},+|\Delta t|) - I(f,\bar{f},-|\Delta t|)}{I(f,\bar{f},+|\Delta t|) + I(f,\bar{f},-|\Delta t|)}$$

$$\approx 4 \ \mathrm{Im}\,\delta_B \frac{\sin\Delta mt}{(1+\cos\Delta mt)}, \qquad (33)$$

and

$$A(f,\bar{f},t) \equiv \frac{J^+(f,\bar{f},t) - J^+(f,\bar{f},t)}{J^+(f,\bar{f},t) + J^+(f,\bar{f},t)}$$

$$\approx 4 \ \mathrm{Im}\,\delta_B \frac{(1-\cos\Delta mt)}{(\Delta mt + \sin\Delta mt)}. \qquad (34)$$

In these equations, direct CPT and $\Delta B = \Delta Q$ violations have been neglected, and $\Delta \gamma t$ and $\Delta \gamma \Delta t$ have been treated as small. The latter holds over the time scales considered and is justified because the lifetime-difference parameter y is small.

For a perfect detector and with the approximations made, Eq. (33) contains a pole structure at $\cos\Delta mt = -1$. This suggests the measured magnitude of the asymmetry is sensitive to precise details of the detector resolution and backgrounds. For this reason, we consider only the asymmetry (34) as an experimental observable for the double-semileptonic case.

The f and $\bar{f}$ states are identified from the sign of the electric charge of the lepton in each semileptonic decay. No dilution of the asymmetry is incurred through flavor mistagging. We take background levels and reconstruction efficiencies from prior works [48]. With an integrated luminosity of 100 fb^{-1}, we expect a sample size of about 2000 reconstructed correlated events with both B^0 mesons decaying semileptonically.

To examine the feasibility of measuring or bounding $\mathrm{Im}\,\delta_B$ using the double-semileptonic channel, we followed a Monte Carlo procedure similar to that used in Sec. III B. Setting $\epsilon_B = 0.045$ and for a range of values of $\mathrm{Im}\,\delta_B$, we produced large samples of 10^6 events incorporating the above experimental effects. We then obtained the asymmetry of Eq. (34) for each sample, allowing for effects due to decay-time resolution resulting in incorrect determination of which B meson decayed first.

Assuming first that $\mathrm{Im}\,\delta_B = 0$, we created an ensemble of 200 datasets of Monte Carlo events, each containing 2000 decays. For the observed $A(f,\bar{f},t)$ distribution in each case, we then performed binned maximum-likelihood fits to the expected shape for a given value of $\mathrm{Im}\,\delta_B$. We thereby obtained an average bound that can be set on $\mathrm{Im}\,\delta_B$.

From the ensemble of 200 datasets that were generated using $\mathrm{Im}\,\delta_B = 0$, the average value of the upper bound on $\mathrm{Im}\,\delta_B$ that can be placed at the 95% C.L. on a single dataset is $\mathrm{Im}\,\delta_B < 0.08$. Figure 4 shows a typical dataset that gives rise to this limit. For the dataset illustrated, the probability is 86% that the data are from a parent distribution with $\mathrm{Im}\,\delta_B = 0$.

Next, we address the more interesting case for which one B meson decays semileptonically while the other decays into $J/\psi K_S$. This is one of the most attractive B-factory channels to determine the angle β in the CKM triangle, using an asymmetry arising between events where the semileptonically tagged B meson decays first and those where the decay into $J/\psi K_S$ occurs first [29]. The exclusive $J/\psi K_S$ decay allows for full reconstruction of the B momentum.

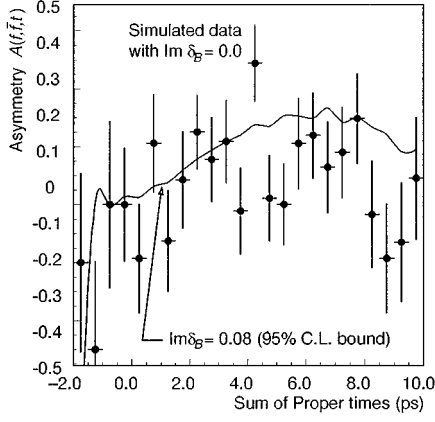For this situation, we can examine two useful asymmetries:

FIG. 4. Simulated data and bound in the double-semileptonic channel at an asymmetric B factory. Points with error bars represent the typical asymmetry $A(f,\bar{f},t)$ as a function of total time t obtained in a Monte Carlo simulation with $\text{Im}\delta_B = 0$ using 2000 correlated $B^0\bar{B}^0$ decays with both mesons decaying into $D^{(*)}\ell\nu$. Superimposed as a solid line is the predicted shape of $A(f,\bar{f},t)$ for $\text{Im}\delta_B = 0.08$, which for this sample is the upper bound at the 95% C.L. determined from the difference of likelihood in binned likelihood fits.

$$A(f,\bar{f},J/\psi K_S,\Delta t)$$

$$\equiv \frac{I(f,J/\psi K_S,\Delta t) - I(\bar{f},J/\psi K_S,\Delta t)}{I(f,J/\psi K_S,\Delta t) + I(\bar{f},J/\psi K_S,\Delta t)}$$

$$\approx 2\,\text{Re}\epsilon_B - 2\,\text{Re}\delta_B - 2(\text{Re}\epsilon_K + \text{Re}\epsilon_B + \text{Re}\delta_K - \text{Re}\delta_B)$$

$$\times \cos\Delta mt + 2(\text{Im}\epsilon_K - \text{Im}\epsilon_B + \text{Im}\delta_K + \text{Im}\delta_B)\sin\Delta mt,$$

$$(35)$$

and

$$A(f,\bar{f},J/\psi K_S,t)$$

$$\equiv \frac{J(f,J/\psi K_S,t) - J(\bar{f},J/\psi K_S,t)}{J(f,J/\psi K_S,t) + J(\bar{f},J/\psi K_S,t)}$$

$$\approx 2\,\text{Re}\epsilon_B - 2\,\text{Re}\delta_B$$

$$-2(\text{Re}\epsilon_K + \text{Re}\epsilon_B + \text{Re}\delta_K - \text{Re}\delta_B)\frac{\sin\Delta mt}{\Delta mt}. \quad (36)$$

In our experimental simulations, we use the asymmetry (36) because it allows a study of $\text{Re}\delta_B$ independent of $\text{Im}\delta_B$.

The procedure we follow is similar to that for the double-semileptonic case. Here, an integrated luminosity of 100 fb^{-1} should result in 2300 reconstructed tagged events [29]. The results of our simulations are illustrated in Fig. 5. If $\text{Re}\delta_B = 0$, an average limit of $\text{Re}\delta_B < 0.035$ at the 95% C.L. can be obtained with a data sample of this size, as is shown in Fig. 5(a). Under the assumption that indirect *CPT* violation with $\text{Re}\delta_B = 0.20$ indeed exists, a typical fit and the associated precisions are illustrated in Fig. 5(b). In the sample indicated, the probability that the simulated dataset is from a parent distribution with $\text{Re}\delta_B = 0$ is less than 0.05%. It may be possible to attain even better sensitiv-
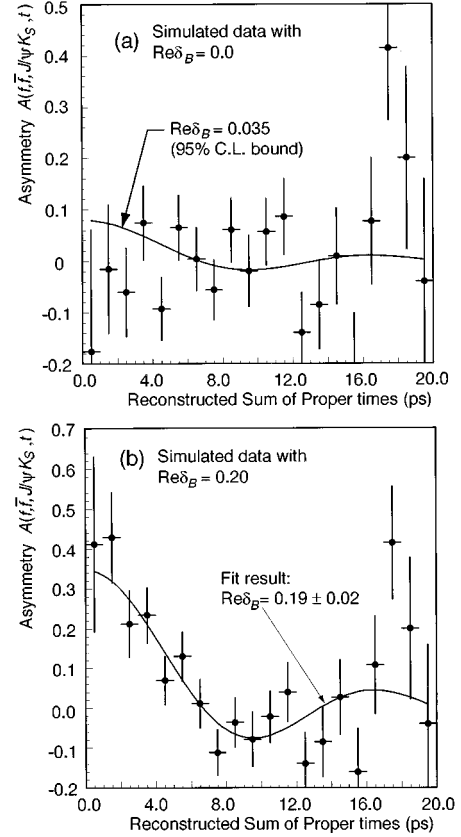

FIG. 5. Simulated data for the semileptonic-$J/\psi K_S$ channel at an asymmetric B factory. (a) Points with error bars represent the typical asymmetry $A(f,\bar{f},J/\psi K_S,t)$ as a function of total time t for a set of 2300 $B^0 \to J/\psi K_S$, $\bar{B}^0 \to D^{(*)}\ell\nu$ correlated decays generated in a Monte Carlo simulation with $\text{Re}\delta_B = 0$. Superimposed as a solid line is the predicted shape for $\text{Re}\delta_B = 0.035$, which for this sample is the upper bound at the 95% C.L. determined from the difference of likelihood in binned likelihood fits. (b) Same as in (a) but for 2300 events generated in a Monte-Carlo simulation with $\text{Re}\delta_B = 0.2$. The solid line is the predicted shape. The fit result and associated precisions are also indicated.

ity by fitting simultaneously to the asymmetry (35) or by performing a full two-dimensional fit to the distributions in t_1 and t_2.

V. SUMMARY

In this paper, we have examined the feasibility of bounding *CPT* violation in the neutral-*B* system. The type of violation allowed might occur in a string scenario within the context of conventional quantum mechanics. Our analysis includes the cases where the mesons are uncorrelated and those where the mesons are correlated and either unboosted or boosted.

On the purely theoretical side, we have provided analytical expressions for both time-dependent and time-integrated decay rates for all these cases, allowing for direct and indirect T and *CPT* violation. Asymmetries are defined that permit the extraction of the parameters for indirect *CPT* viola-

tion. To address the issue of experimental testing of these effects, we have performed Monte Carlo simulations to model various plausible experimental situations. Both data already taken and data likely to be available within a few years are considered. Our treatment incorporates background effects and acceptances appropriate for the detectors OPAL at CERN, CLEO at CESR, and BaBar at SLAC.

At present, no bounds exist on CPT violation in the B system. Our analysis suggests that under reasonable assumptions and *with data already available* a bound of order 10% can be placed on CPT-violation parameter δ_B. Our simulations also suggest that the CPT reach of planned experiments is likely to attain the level of a few percent within the near future.

Given the role of CPT invariance as a fundamental symmetry of the standard model, testing it is vital. If CPT violation were discovered, it could provide a test of string theory and in any event would have far-reaching implications for our understanding of nature.

---

[1] J. Schwinger, Phys. Rev. **82**, 914 (1951).

[2] G. Lüders, Det. K. Dan. Vidensk. Selsk. Mat.-Fys. Medd. **28** (5) (1954); Ann. Phys. (N.Y.) **2**, 1 (1957).

[3] J.S. Bell, thesis, Birmingham University 1954; Proc. R. Soc. London **A231**, 479 (1955).

[4] W. Pauli, in *Niels Bohr and the Development of Physics*, edited by W. Pauli (McGraw-Hill, New York, 1955), p. 30.

[5] G. Lüders and B. Zumino, Phys. Rev. **106**, 385 (1957).

[6] R.F. Streater and A.S. Wightman, *PCT, Spin and Statistics, and All That* (Benjamin Cummings, Reading, 1964).

[7] R. Jost, *The General Theory of Quantized Fields* (AMS, Providence, 1965).

[8] V.A. Kostelecký and R. Potting, Nucl. Phys. **B359**, 545 (1991); Phys. Lett. B **381**, 89 (1996).

[9] See also V.A. Kostelecký, R. Potting, and S. Samuel, in *Proceedings of the Joint International Lepton-Photon Symposium and Europhysics Conference on High Energy Physics*, Geneva, Switzerland, 1991, edited by S. Hegarty, K. Potter, and E. Quercigh (World Scientific, Singapore, 1992); V.A. Kostelecký and R. Potting, in *Gamma Ray-Neutrino Cosmology and Planck Scale Physics*, edited by D. B. Cline (World Scientific, Singapore, 1993), Report No. hep-th/9211116.

[10] V.A. Kostelecký and R. Potting, Phys. Rev. D **51**, 3923 (1995).

[11] S.W. Hawking, Phys. Rev. D **14**, 2460 (1976); Commun. Math. Phys. **87**, 395 (1982); Phys. Rev. D **32**, 2489 (1985).

[12] D. Page, Phys. Rev. Lett. **44**, 301 (1980); Gen. Relativ. Gravit. **14**, 299 (1982); Phys. Rev. D **32**, 2496 (1985).

[13] R.M. Wald, Phys. Rev. D **21**, 2742 (1980).

[14] J. Ellis, N.E. Mavromatos, and D.V. Nanopoulos, Int. J. Mod. Phys. A **11**, 1469 (1996); see also J. Ellis, J.L. Lopez, N.E. Mavromatos, and D.V. Nanopoulos, Phys. Rev. D **53**, 3846 (1996).

[15] R. Carosi *et al.*, Phys. Lett. B **237**, 303 (1990).

[16] M. Karlsson *et al.*, Phys. Rev. Lett. **64**, 2976 (1990).

[17] L.K. Gibbons *et al.*, Phys. Rev. Lett. **70**, 1199 (1993).

[18] CPLEAR Collaboration, T. Ruf, in *Proceedings of the XXVII International Conference on High Energy Physics*, Glasgow, Scotland, 1994, edited by P.J. Bussey and I.G. Knowles (IOP, London, 1995).

[19] D. Colladay and V.A. Kostelecký, Phys. Lett. B **344**, 259 (1995).

[20] D. Colladay and V.A. Kostelecký, Phys. Rev. D **52**, 6224 (1995).

[21] M. Kobayashi and A.I. Sanda, Phys. Rev. Lett. **69**, 3139 (1992).

[22] Z.-Z. Xing, Phys. Rev. D **50**, 2957 (1994).

[23] This is taken to the official end date of the LEP program running at the Z^0 resonance, October 1996.

[24] For example, CDF has collected samples of 872 $B^0 \to D^{(*)}\ell\nu$ events in a dataset of 19.3 pb^{-1} [CDF Collaboration, F. Abe *et al.*, Phys. Rev. Lett. **76**, 4307 (1996)]; and 285 $B^0 \to J/\psi K_S$ events in a data set of 67.7 pb^{-1} [J. Kroll, in the Proceedings of the Symposium on Lepton-Photon Interactions, Beijing, China, 1995 (unpublished)].

[25] See, for example, CLEO Collaboration, J.E. Duboscq *et al.*, Phys. Rev. Lett. **76**, 3898 (1996).

[26] BELLE Collaboration, M.T. Cheng *et al.*, Letter of Intent for a Study of CP Violation in B Meson Decays, KEK-94-2, 1994 (unpublished); BaBar Collaboration, D. Boutigny *et al.*, Letter of Intent for the Study of CP Violation and Heavy Flavor Physics at PEP-II, SLAC-0443, 1994 (unpublished).

[27] OPAL Collaboration, K. Ahmet *et al.*, Nucl. Instrum. Methods Phys. Res. A **305**, 275 (1991); J. Allison *et al.*, *ibid.* **317**, 47 (1992).

[28] The CESR CLEO Upgrade Project, CLNS-93-1265, 1994.

[29] BaBar Collaboration, D. Boutigny *et al.*, BaBar Technical Design Report, SLAC-R-95-457, 1995 (unpublished).

[30] Particle Data Group, L. Montanet *et al.*, Phys. Rev. D **50**, 1173 (1994), and 1995 off-year partial update for the 1996 edition available on the PDG WWW pages (URL: http://pdg.lbl.gov/).

[31] Unless otherwise noted, all references to the B^0 meson in this work refer to the B_d^0, although much of the theoretical framework applies also to the B_s^0.

[32] L.-L. Chau, Phys. Rep. **95**, 1 (1983).

[33] P.J. Franzini, Phys. Rep. **173**, 1 (1989).

[34] E.A. Paschos and U. Turke, Phys. Rep. **178**, 145 (1989).

[35] I.I. Bigi, in *CP Violation and Beauty Factories*, edited by D.B. Cline and A. Fridman [Ann. N.Y. Acad. Sci. **619** (1991)].

[36] T.D. Lee and C.S. Wu, Annu. Rev. Nucl. Sci. **16**, 511 (1966).

[37] V.V. Barmin *et al.*, Nucl. Phys. **B247**, 293 (1984).

[38] N.W. Tanner and R.H. Dalitz, Ann. Phys. (N.Y.) **171**, 463 (1986).

[39] T. Sjöstrand, The JETSET 7.3 Manual, CERN-TH.6488/92 (un-

published); Comput. Phys. Commun. **39**, 347 (1987); T. Sjöstrand and M. Bengtsson, *ibid.* **43**, 367 (1987).

[40] OPAL Collaboration, R. Akers *et al.*, Z. Phys. C **67**, 379 (1995).

[41] OPAL Collaboration, R. Akers *et al.*, Phys. Lett. B **336**, 585 (1994).

[42] ALEPH Collaboration, D. Buskulic *et al.*, Phys. Lett. B **313**, 498 (1993); **322**, 441 (1994).

[43] In a complete experimental analysis, either a measured value of ϵ_B must be used or fits with varying ϵ_B must be performed.

[44] This is chosen from the limit $|\mathrm{Re}\,\epsilon_B| < 0.045$ at 90% C.L., CLEO Collaboration, J. Bartelt *et al.*, Phys. Rev. Lett. **71**, 1680 (1993). Taking other values for ϵ_B below this limit would not significantly affect the bounds and fits on δ_B obtained in the present paper.

[45] ALEPH Collaboration, D. Buskulic *et al.*, Improved Measurement of the $\overline{B}^0$ and B^- Meson Lifetimes, CERN-PPE-96-014, 1996 (unpublished).

[46] C.S. Mishra, in *The Fermilab Meeting*, Proceedings of the Meeting of the Division of Particles and Fields of the APS, Batavia, Illinois, 1992, edited by C.H. Albright *et al.* (World Scientific, Singapore, 1993).

[47] The CLEO III Detector: Design and Physics Goals, 1994 (unpublished), available from the World Wide Web page: http://w4.lns.cornell.edu/public/CLEO/CLEO3/CLEO3.html.

[48] CLEO Collaboration, B. Barish *et al.*, Phys. Rev. Lett. **76**, 1570 (1996); CLEO Collaboration, B. Barish *et al.*, Phys. Rev. D **51**, 1014 (1995).

[49] CLEO Collaboration, M. Alam *et al.*, Phys. Rev. D **50**, 43 (1994).